Civil Engineering Dimension
https://ced.petra.ac.id

Seismic Performance Evaluation of An Interior Reinforced Concrete Beam-Column Joint Subjected to Cyclic Loading

Chandra, J.[1]*, **Wibowo, H.**[2], **Christian, Y.B.**[1], **Handoko, J.**[1], **Gunawan, A.**[1], **and Ardenlie, F.G.**[1]
[1] Civil Engineering Department, Faculty of Civil Engineering and Planning, Petra Christian University, Jl. Siwalankerto 121-131, Surabaya 60236, INDONESIA
[2] Department of Civil, Construction, and Environmental Engineering, Iowa State University, 813 Bissell Road, Ames, Iowa, UNITED STATES OF AMERICA

DOI: https://doi.org/10.9744/ced.27.2.180-192

Article Info:
Submitted: Apr 15, 2025
Reviewed: May 09, 2025
Accepted: Aug 22, 2025

Keywords:
reinforced concrete (RC),
beam-column joint,
code provisions,
bond-slip,
hysteretic behavior.

Corresponding Author:
Chandra, J.
Civil Engineering Department, Faculty of Civil Engineering and Planning, Petra Christian University, Jl. Siwalankerto 121-131, Surabaya 60236, INDONESIA
Email: Chandra.jimmy@petra.ac.id

Abstract

Many reinforced concrete (RC) buildings in Indonesia suffered severe earthquake damages due to brittle failure and poor detailing works of the beam-column joints. This experimental study aims to investigate the seismic performance of an interior beam-column joint designed according to ACI 318-19 code provisions. The specimen was subjected to static axial loading to simulate gravity loading on column and lateral quasi-static cyclic loading to simulate earthquake loading. From the experimental results, it shows that the RC beam-column joint exhibited ductile beam flexural failure as expected. However, there was a considerable bond-slip noticed on beam's longitudinal reinforcement. In addition to the experimental study, a finite element analysis was also performed using VecTor2 software. The analysis results show that the model could simulate well the hysteretic behavior of the specimen. Furthermore, from the analysis, bond-slip was also found to be a key factor affecting the hysteretic behavior of the joint.

INTRODUCTION

Beam–column joints are important elements in reinforced concrete (RC) special moment-resisting frames that affects their seismic performance. Beam-column joints transfer forces and moments between beams and columns due to the imposed lateral forces and need to be designed accordingly. Capacity design philosophy allows plastic hinges to occur in RC special moment-resisting frames to accommodate large displacements due to earthquake loadings. These plastic hinges are expected to occur at the beam ends and they will experience significant inelastic rotations during earthquakes [1]. In capacity design philosophy, the columns are designed to be stronger than the beams and thus damage will be concentrated on the beams while keeping the columns and joints less damaged. Moreover, to achieve the desired performance for beam-column joints, attention should be given to the reinforcement detailing. Adequate ductility of the joints can be achieved by providing sufficient confinement reinforcement and thus allowing the beams to yield at the faces of the columns [1]. However, many RC buildings, especially in Indonesia, still suffered severe earthquake damages mainly due to substantially brittle failure and poor detailing works of the beam-column joints [2].

Another factor affecting beam-column joints' seismic performance is bond-slip that occurs in beam's longitudinal reinforcement [3]. ACI 318-19 [4] specifies that joint depth of special moment-resisting frames shall be at least 20 times of greatest beam's bar diameter (d_b) for interior beam-column joints. This provision has not been changed since ACI 318-83 [5]. In addition, this provision was supported by the research from Zhu and Jirsa [6]. They concluded

Note : Discussion is expected before November, 1st 2025, and will be published in the "Civil Engineering Dimension", volume 28, number 1, March 2026.
ISSN : 1410-9530 print / 1979-570X online
Published by : **Petra Christian University**

that there was no substantial loss of strength and bond damage observed at interstory drift of 0.03 for interior beam-column joints having joint depth more than 17 d_b. However, an experimental study by Leon [3] suggested that the provision was adequate for moderate earthquakes but it might lead to considerable stiffness and strength losses under major earthquakes. In the study, Leon [3] investigated four beam-column joint specimens with variation in joint depth (16, 20, 24, and 28 d_b). The experiment results showed that bond efficiencies were 64%, 71%, 86%, and 97% for specimens having joint depth of 16, 20, 24, and 28 d_b, respectively. Based on this study, Leon [3] suggested that joint depth of 24 d_b was the ideal anchorage length for interior beam-column joints.

This current study focuses on investigating the seismic performance of an interior beam-column joint designed according to ACI 318-19 [4] provisions by performing an experimental study at the Structural Engineering Laboratory of Petra Christian University, Indonesia. Subsequently, the tested specimen was evaluated using ACI 374.1-05 [7] criteria for RC special moment-resisting frames. In addition, the hysteretic curve obtained from the experiment was also compared with results from finite element analysis using VecTor2 software [8]. It is expected that this study could provide more insight into the seismic behavior of interior RC beam-column joints, especially regarding the bond-slip behavior.

EXPERIMENTAL PROGRAM

An interior RC beam-column joint was tested in this experimental program which was subjected to static axial loading to simulate gravity loading on column and lateral quasi-static cyclic loading to simulate earthquake loading. The beam width and height are 250 mm and 400 mm, respectively, whereas the column dimension used is 400 mm × 400 mm. The total lengths of the beam and column are 4000 mm and 2760 mm, respectively. The specimen details can be seen in Figure 1. The concrete compressive strength used was 31.4 MPa whereas the steel material properties can be seen in Table 1. It is worth noting that the specimen's joint depth (400 mm which is about 21 times diameter of beam's bar) is slightly above the minimum requirement in the ACI 318-19 [4] code.

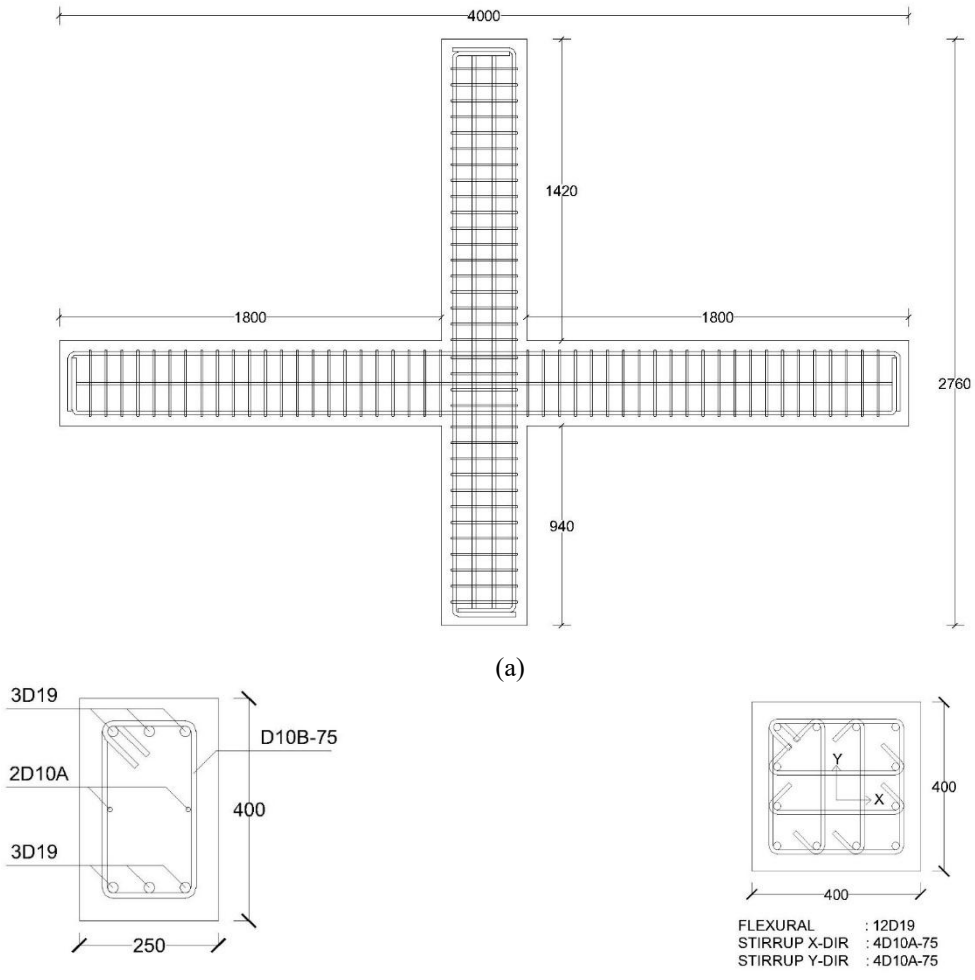

Figure 1. (a) Overall Dimensions; (B) Beam and (C) Column Reinforcement Details of The RC Beam-Column Joint Specimen Tested in This Study. All Dimensions are in Millimeters

Table 1. Properties of Steel Bars Used in This Study

Rebar	Code	f_y	f_u	f_y average	f_u average	ε_y average	ε_u average	E average
		[MPa]	[MPa]	[MPa]	[MPa]	[mm/mm]	[mm/mm]	[MPa]
D19	1	483.25	624.97	477.18	644.76	0.00262	0.10229	221582
	2	474.52	654.14					
	3	473.79	655.16					
D10 - A	A1	552.71	1006.83	510.32	1013.04	0.00200	0.08395	228349
	A2	521.91	1023.92					
	A3	456.36	1008.37					
D10 - B	B1	457.17	649.07	437.40	652.70	0.00261	0.12263	197836
	B2	421.12	657.62					
	B3	433.92	651.40					

The specimen was designed according to ACI 318-19 [4] code for RC special moment-resisting frames. Based on the code, the columns were designed to be stronger than the beams and hence damages were expected to be concentrated on the beams while keeping the columns and joint less damaged. Furthermore, to achieve the desired performance for the RC beam-column joint, i.e. beam flexural failure, sufficient confinement reinforcements were provided at the beams, columns, and joint. This helped the RC beam-column joint to maintain its ductility under reversal lateral loading. The calculated strength values of the beams, columns, and joint based on actual material properties can be seen in Table 2.

Test Setup

The specimen was restrained with pin support at the bottom of the column and the beams were restrained for vertical movement at the inflection points (see Figure 2). Cyclic lateral force was generated by a double-acting hydraulic cylinder attached to the top of the column. In addition, vertical hydraulic cylinders and spreader beam were used to apply axial force to the column. There was a total of five load cells (LC) used in the experiment. LC1 was placed in front of the lateral hydraulic cylinder to measure the generated lateral load, while LC2 and LC3 were placed above the vertical hydraulic cylinders to measure the generated axial load. LC4 and LC5 were placed below the beams to measure their vertical reactions.

Table 2. Actual Theoretical Strength Values of The Specimen

Member	Parameter	Value	Unit
Beam	M_{crack}	23.16	(kNm)
	M_n	125.86	(kNm)
	M_{pr}	153.47	(kNm)
Column	M_{crack}	37.06	(kNm)
	M_n	317.00	(kNm)
	M_{pr}	342.40	(kNm)
Joint	V_j	893.54	(kN)
	ϕV_n	952.61	(kN)

Figure 2. Overall Test Setup of the RC Beam-column Joint Specimen

Instrumentation

A data logger was used to record data obtained during the experiment such as specimen's deflections measured by linear variable displacement transformers (LVDTs) and strains in steel bars measured by strain gauges. There were twenty LVDTs used in this experiment. DT1 to DT5 gave the drift data of the specimen due to the lateral load. DT6 was used to measure any movement of the pin support at the bottom of the column. DT7 to DT10 were used to measure column's flexural deformation, whereas DT11 to D18 were used to measure beam's flexural deformation. Lastly, DT19 and DT20 were used to measure joint shear deformation. The LVDTs setup for this experiment can be seen in Figure 3.

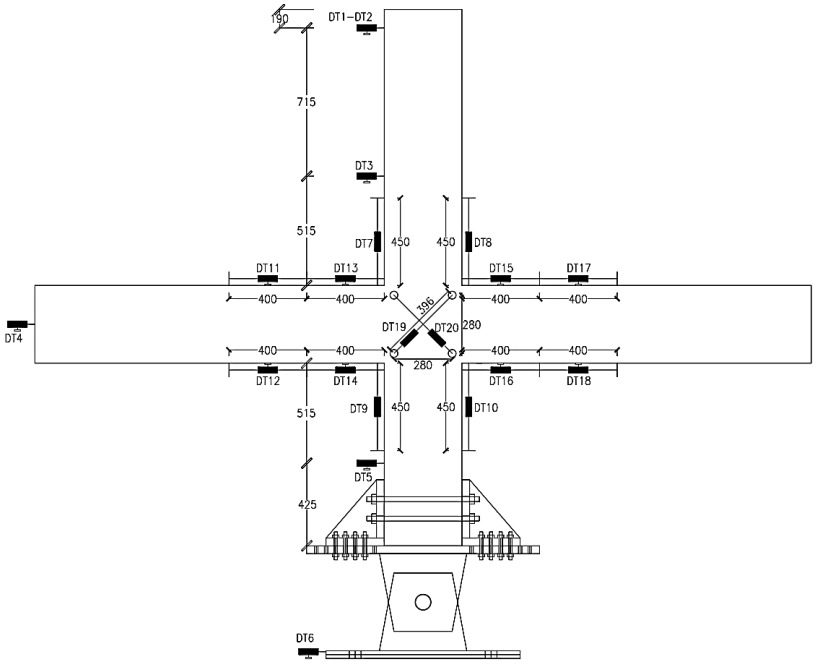

Figure 3. LVDTs Setup of The Specimen

In this experiment, there were twenty-six strain gauges used to measure steel bars' strains. SG1 to SG10 were placed on the column's longitudinal reinforcements at the extreme tension or compression sides, while SG11 to SG24 were placed on the beam's top and bottom longitudinal reinforcements. These strain gauges were installed in the middle reinforcements which were closest to the column/beam axes. Some strain gauges were located close enough to the joint to observe reinforcements yielding in the region of maximum moment. Furthermore, some strain gauges were located inside the joint to measure strain profile within the joint. The strain gauges setup in this experiment is shown in Figure 4.

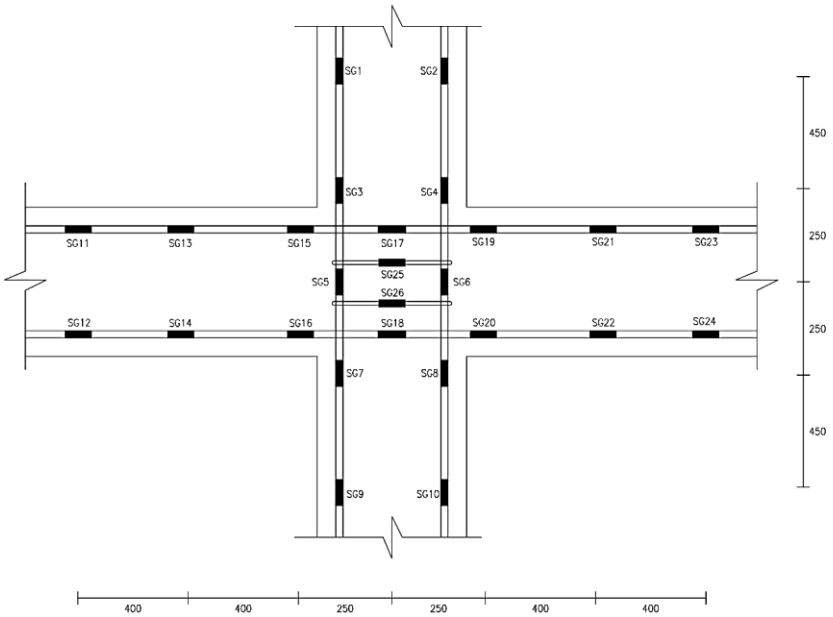

Figure 4. Strain Gauges Setup of The Specimen

Test Procedure

An axial force of 754 kN (equals to $0.15A_g f'_c$) was applied initially to the RC column using the vertical hydraulic cylinders and spreader beam. This value was selected since it was within the possible range of axial load for RC columns in general buildings. The lateral cyclic loading was applied using the horizontal hydraulic cylinder with displacement controller. The loading history used in this experiment can be seen in Figure 5. Each cycle has positive and negative drift amplitudes which were applied three times before they were increased gradually for the subsequent cycles. The specimen was planned to be loaded up to 6% drift ratio. At each drift amplitude, crack patterns were drawn to observe crack propagations of the specimen during testing.

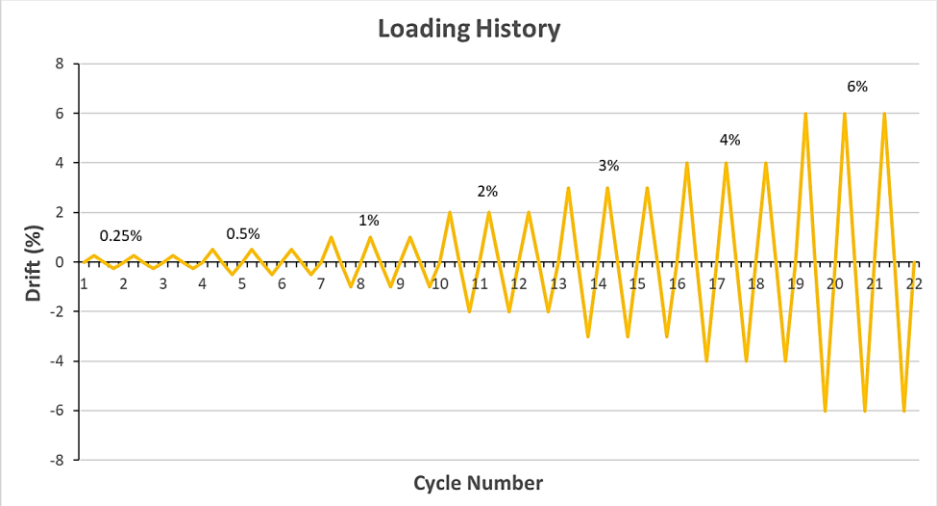

Figure 5. Loading History Used in This Experiment

FINITE ELEMENT ANALYSIS

Macro or micro modeling can be used to develop a finite element model of the RC beam-column joint. Macro modeling that utilizes frame elements with plastic hinges is less detailed, but it has faster computational time compared to micro modeling. Thus, it is mostly used to perform larger scale analysis such as nonlinear dynamic time history. On the other hand, micro modeling is based on the distributed plasticity model, and it could capture the structural responses more accurately. Nevertheless, it requires longer computational time and adequate computing devices as compared to macro modeling.

In this study, micro modeling was chosen to be implemented because this research aims to capture the inelastic responses of the RC beam-column joint at the element level. The nonlinear finite element analysis was conducted using Version 4.4 of VecTor2 Basic [8] computer software. VecTor2 is a software developed to perform nonlinear finite element analysis of two-dimensional RC membrane elements. This software is based on the Modified Compression Field Theory (MCFT) by Vecchio and Collins [9] and Disturbed Stress Field Model (DSFM) by Vecchio [10]. VecTor2 has the capability to predict the force-deformation response of RC structures subjected to static monotonic and reversed cyclic loadings [11].

Material Properties

In this study, concrete material used in VecTor2 was the basic concrete model that is based on Hognestad Parabola and Kent-Park model [12]. The typical stress-strain curve of the concrete material is shown in Figure 6a. Moreover, the model proposed by Seckin [13] was used to define the stress-strain curve for reinforcement material. Based on the VecTor2 manual [11], this model is provided in two options, i.e., Seckin with Bauschinger-Trilinear and Seckin with Bauschinger-HP4. By default, the typical stress-strain curve of the reinforcement material using Seckin [13] with Bauschinger model is shown in Figure 6b.

Bond-Slip Properties

Bond stress is the stress acting on the surface between reinforcement and concrete and the direction is parallel to the rebar. A perfect bond condition means that the displacement of nodal points are the same for both concrete and

reinforcement [14]. Nevertheless, this condition is only applicable in region with low stress between concrete and reinforcement. In the region near cracks, there is possibility of high stress between concrete and reinforcement, and hence bond-slip may occur. In order to achieve more accurate prediction of the bond-slip condition, an additional element at the interface between concrete and reinforcement needs to be introduced. In this study, the bond stress-slip curve is defined using Eligehausen et al. model [15] and the typical curve can be seen in Figure 7.

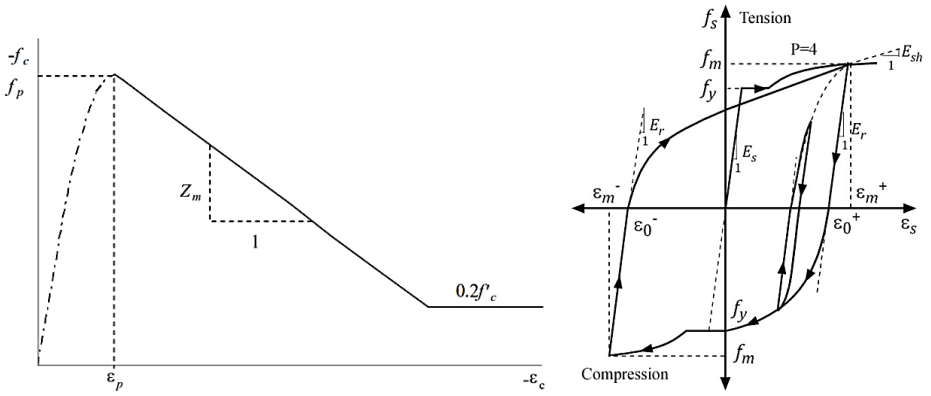

Figure 6. Typical Stress-Strain Curve of Materials Used in this Study [11]

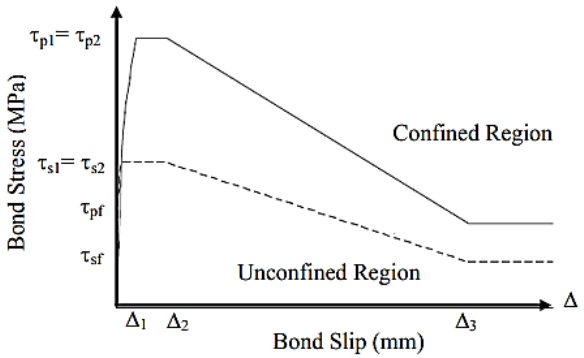

Figure 7. Typical Bond Stress-Slip Curve Used in this Study [11]

Finite Element Modeling

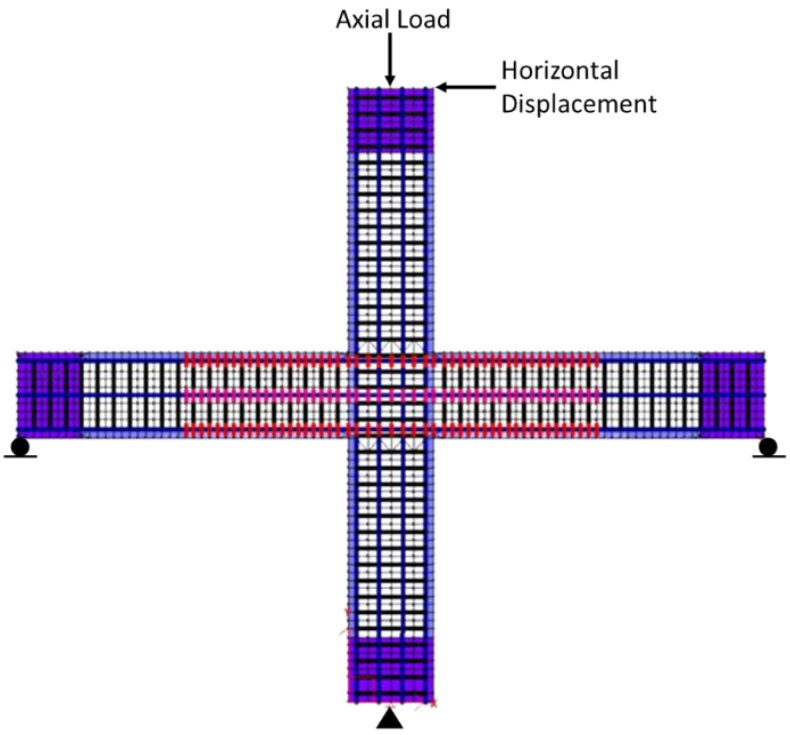

Figure 8. Finite Element Model of The RC Beam-Column Joint Specimen

A total of 1380 rectangular elements and 84 triangular elements with 50 x 50 mm mesh size were used to model the specimen in this study. Furthermore, a total of 1118 truss elements and smeared reinforcements were used to model the longitudinal and transverse reinforcements. In addition, a total of 147 link elements were also used to represent the bond-slip behavior of the specimen. The boundary conditions were modeled with pin support at the bottom of the column and roller supports at the beam ends following the experimental test setup. Moreover, load cases 1 and 2 were assigned to apply axial loading and lateral cyclic loading, respectively. The details of the specimen's finite element model can be seen in Figure 8.

EXPERIMENTAL AND ANALYTICAL RESULTS

This section presents the results of RC beam-column joint experimental testing and discusses the performance of the joint based on ACI 374.1-05 [7] acceptance criteria for RC special moment-resisting frames. In addition, the results from the experimental study will also be compared to analytical results from VecTor2 software [8].

Crack Patterns and Force-Drift Relationship

Cycle No. +03; +0.25%; +22 kN

Cycle No. -06; -0.50%; -36 kN

Cycle No. +09; +1.00%; +69 kN

Cycle No. -12; -2.00%; -105 kN

Cycle No. +18; +4.00%; +97 kN

Cycle No. -21; -6.00%; -63 kN

Figure 9. Crack Patterns Propagation of the RC beam-column Joint Specimen during Testing. Note: +18; +4.00%; +97 kN indicates the eighteenth cycle in positive direction, drift ratio, and lateral force at the respective drift ratio. Positive direction is from left to right

The force-drift ratio curve of the specimen is shown in Figure 10. It is shown that the first crack in beams occurred as early as 0.25% drift and followed by column and joint first crack at 1.00% drift. The flexural reinforcement at beams started to yield at about 1.50% drift and the respective lateral force recorded was very close to the lateral force value that corresponds to actual theoretical nominal moment strength of the beams. Moreover, joint stirrup also started to yield at about 2.50% drift. The recorded maximum force and associated drift ratio are +120 kN and +3.00%, respectively. The maximum force recorded was very close to the lateral force value that corresponds to actual theoretical probable moment strength of the beams. The specimen failed in ductile beam flexural failure at the second cycle of 6.00% drift where the lateral force dropped below 75% of the maximum lateral force recorded. This was caused by crushing of the compression zone at beam ends as well as spalling of cover concrete at columns near major diagonal cracks.

The crack patterns propagation is shown in Figure 9. The first numbers represent cycle numbers in the positive or negative directions. The second and third notations denote respective drift ratios and lateral forces. In the beginning of testing until 0.50% drift, flexural cracks only appeared at the beams. As the drift increased, the number of cracks in beams also increased. Moreover, at 1.00% drift, some flexural cracks were also observed in columns and there were diagonal cracks in the joint. These major diagonal cracks became more apparent at 4.00% drift. At the end of the testing, i.e. 6.00% drift, crushing of the compression zone at the beam ends were spotted and there were spalling of cover concrete at columns near major diagonal cracks.

Deformation Contributions and Strains

The horizontal displacement generated by lateral load applied consists of deformations of the beams, columns, and joint. The beam deformation consists of elastic and plastic flexural deformations while the column deformation consists of elastic flexural deformation since there was no yielding of reinforcement at columns observed during testing. The joint deformation consists of joint shear deformation. The deformations from beam shear and column shear were regarded as uncounted deformations. Figure 11 shows the deformation contributions of these deformation components to total lateral drift. In the early stage of loading until 1.00% drift, joint shear deformation was very low since there was no diagonal crack occurred in the joint. Starting from 2.00% drift onwards, joint shear deformation became more significant with the occurrence of diagonal cracks and yielding of stirrups at the joint. On the other hand, contribution of beam elastic flexural deformation decreased as the drift increased. This was because the longitudinal reinforcement in beams yielded and thus the beams entered plastic stage starting from 1.50% drift onwards. Overall, beam flexural deformations dominated the deformation components of the specimen and column flexural deformation was low since there was no yielding of reinforcement at columns. This emphasizes that the specimen failed in beam flexural failure.

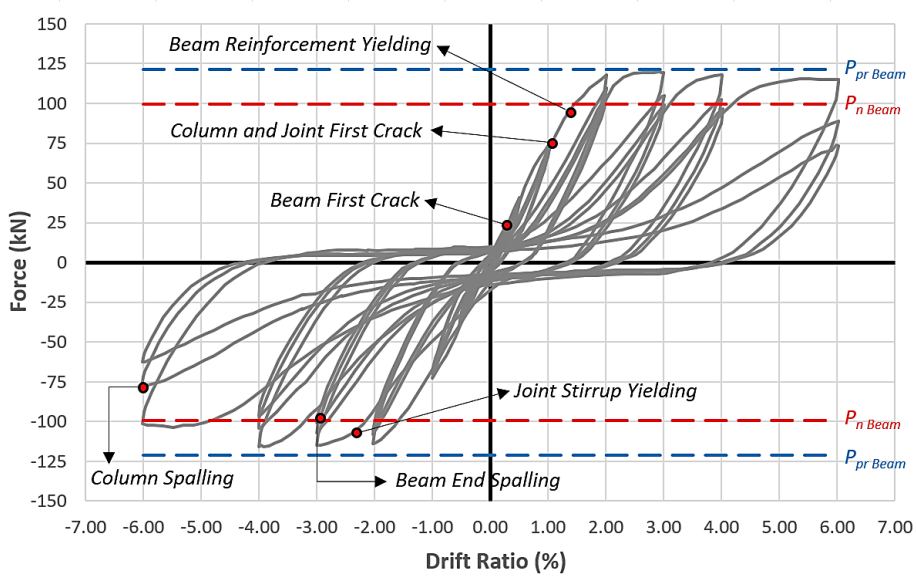

Figure 10. Force-drift Ratio Curve of the Specimen

The strain distributions in beam top reinforcement and column longitudinal reinforcement are shown in Figure 12. These strains were recorded to observe whether the steel reinforcements had yielded during experimental testing and they were plotted at the drift amplitudes. At the initial stage, the strains in beam and column reinforcements were

still low and these values gradually increased with increment of the drift amplitudes. At drift ratio of 2.00%, it was found that beam top reinforcement located near the column had yielded. The strain values increased greatly at subsequent drift amplitudes and hence the beam top reinforcement strain values could only be obtained until 3.00% drift ratio. At this ratio, considerable bond-slip at beam top reinforcement was noticed. On the other hand, strain values in column longitudinal reinforcement were below yield strain during the testing (up to 6.00% drift) and thus it can be concluded that strong column-weak beam behavior was indeed portrayed in the specimen.

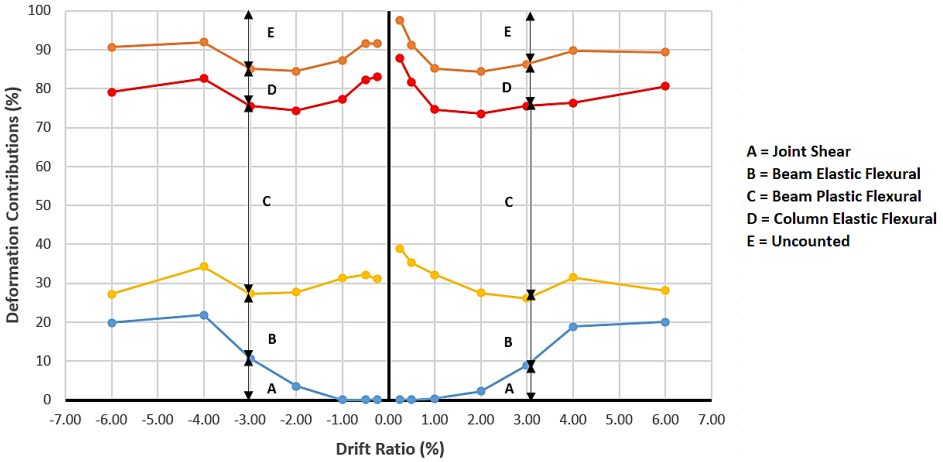

Figure 11. Contributions of RC Beam-column Joint Deformation Components to Total Drift

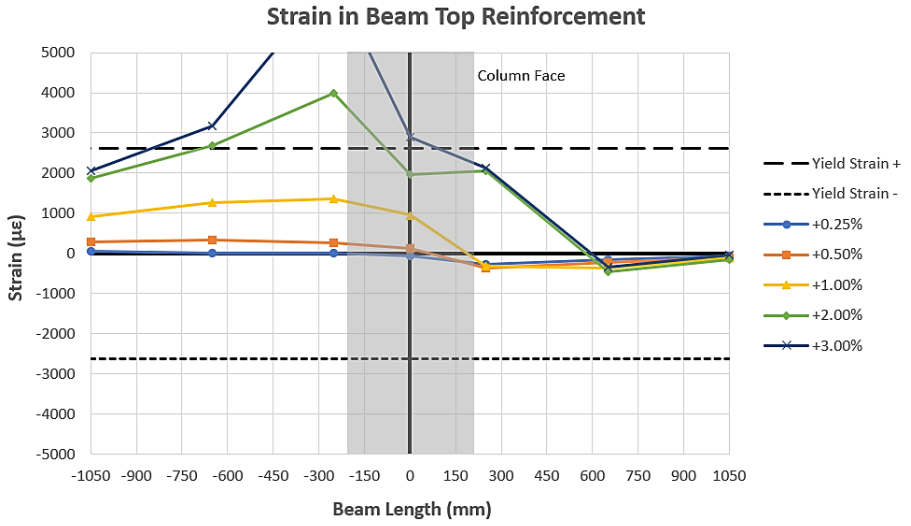

(a)

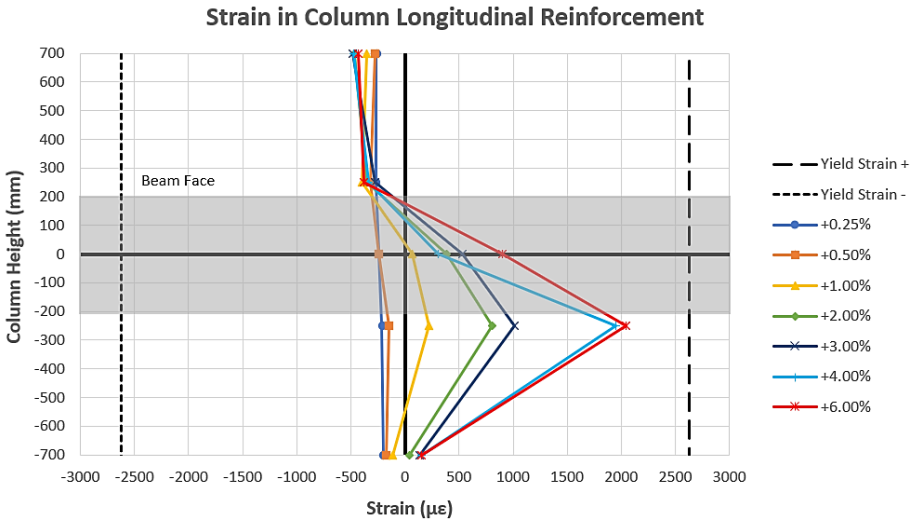

(b)

Figure 12. Strain Distributions in a) Beam Top Reinforcement; b) Column Longitudinal Reinforcement

Seismic Performance Evaluation of The Specimen

To evaluate the seismic performance of the RC beam-column joint specimen, ACI 374.1-05 [7] specifies the following criteria; 1) load-carrying capacity and strength degradation, 2) energy dissipation ratio, and 3) the residual stiffness at or after the third cycle of 3.50% drift ratio. In this experiment, the evaluation was done on the third cycle of 4.00% drift ratio (cycle no. 18).

The maximum forces applied to the specimen were 120 kN and -116 kN in positive and negative directions, respectively. ACI 374.1-05 [7] specifies that the maximum lateral resistance of the specimen should not exceed the nominal capacity of the test column to ensure strong column-weak beam behavior. In this study, the lateral force that corresponds to the actual moment capacity of the column is 257.72 kN. Thus, as the maximum force of the specimen did not exceed this value, the specimen satisfied the strong column-weak beam design principle. It is worth noting that the nominal moment capacity of columns is about 2.5 times greater than that of beams. Furthermore, ACI 374.1-05 [7] specifies that strength degradation of a special moment resisting frame to be maximum 25% of the peak load in each direction at the third cycle of 3.50% drift ratio. In this study, the maximum forces at the third cycle of 4.00% drift ratio were 96.50 kN and -96.50 kN for positive and negative directions, respectively. Hence, the strength degradations were below 25% of the peak loads.

Energy dissipation increases as the drift ratio increases. The energy dissipation values are at the highest in the first cycle but decrease in the second and third cycles due to the strength degradation. ACI 374.1-05 [7] specifies that the relative energy dissipation ratio of the test specimen after the third cycle of 3.50% drift ratio should not be less than 0.125. As shown in Figure 13, the specimen satisfied this criteria.

The initial and residual stiffness were obtained from the force-displacement curve of the specimen as illustrated in Figure 14. The initial stiffness (Ki) was determined as a direct division of the first cycle of 0.50% drift ratio peak load to its displacement. The residual stiffness (K0) was taken as the secant stiffness between displacement of ±10% of the third cycle of 4.00% drift ratio. ACI 374.1-05 [7] specifies that the residual stiffness for both directions should be greater than 5% of the initial stiffness. However, in this study, the residual stiffness of the specimen were only 4.4% and 4.7% of the initial stiffness for positive and negative directions, respectively. This means the specimen did not satisfy the ACI 374.1-05 [7] criteria for residual stiffness.

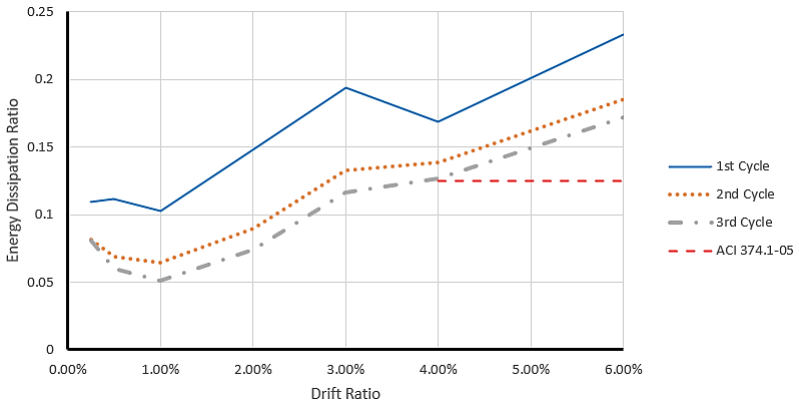

Figure 13. Relative Energy Dissipation Ratio of The Tested Specimen

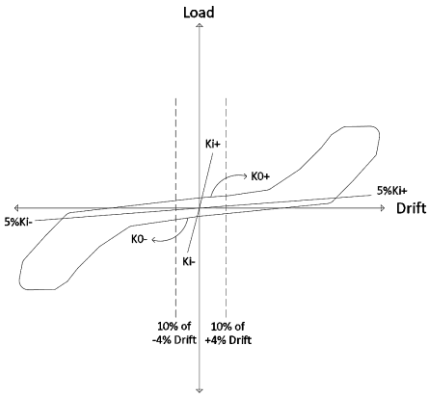

Figure 14. Residual Stiffness Evaluation

Comparison between Experimental and Analytical Results

Figure 15 shows the comparison of the RC beam-column joint specimen's hysteretic curves obtained from the experiment and finite element analysis using VecTor2 software [8]. Generally, it can be observed that the finite element model could predict well the hysteretic behavior of the specimen, including strength degradation in subsequent cycles and pinching behavior. Furthermore, the model could predict accurately the peak lateral forces of the specimen in both directions. Figure 16 shows the comparison of crack patterns between the experiment and finite element analysis. From the figure, it can be seen that the finite element model could capture reasonably well the crack patterns of the specimen, including concrete crushing at beams' end and cracks at column and joint areas.

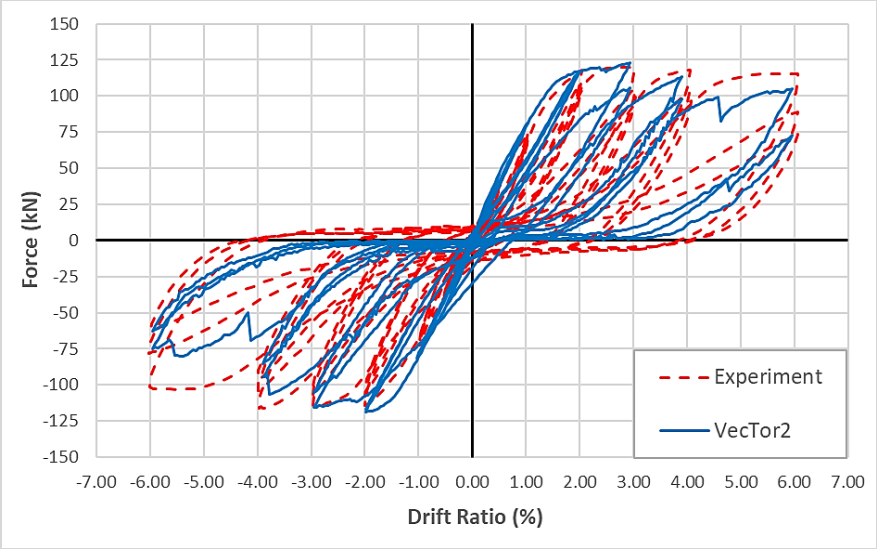

Figure 15. Comparison of RC Beam-column Joint Specimen's Hysteretic Curves Obtained from The Experiment and Finite Element Analysis

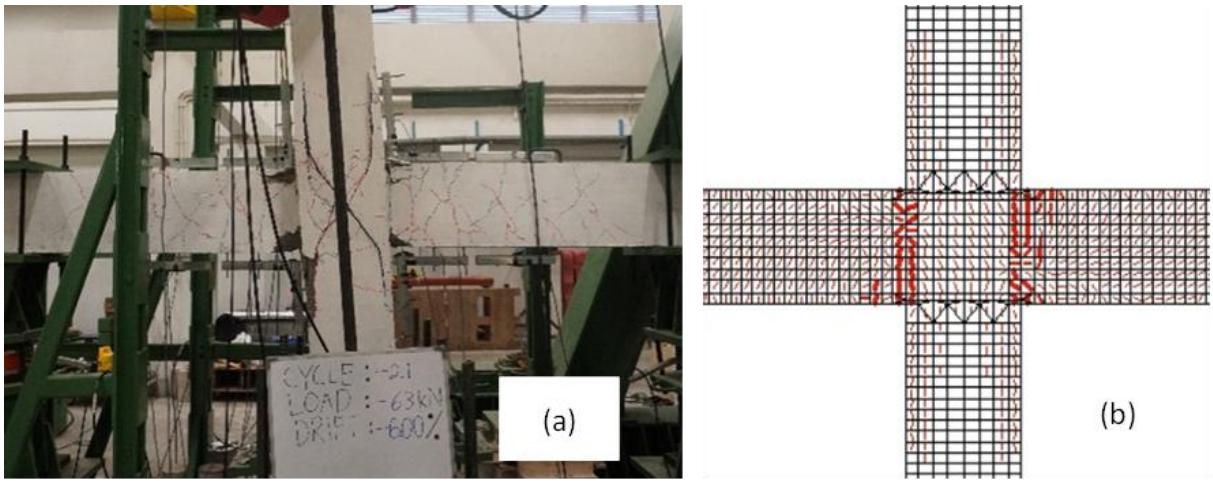

Figure 16. Comparison of RC Beam-column Joint Specimen's Crack Patterns Obtained from a) The Experiment; and b) Finite Element Analysis

Discussions

The RC beam-column joint specimen in this study was designed according to ACI 318-19 [4] code for RC special moment-resisting frames. The experiment results show that the specimen exhibited beam flexural failure, and it demonstrated clearly strong column-weak beam behavior. It should be noted that the ratio of actual theoretical value of column nominal moment capacity to beam nominal moment capacity was about 2.5, which this is more than two times required by ACI 318-19 [4] code. This was done so that the columns were not damaged or yielded during the experiment. Hence, bond-slip in the specimen was expected to occur only in beam's reinforcement.

According to acceptance criteria of ACI 374.1-05 [7] for RC special moment-resisting frames, the specimen satisfied all criteria except the residual stiffness. The residual stiffness was slightly less than 5% of initial stiffness as required

by the code. The significant pinching behavior of the specimen was due to bond-slip that happened in beam's longitudinal reinforcement as shown in Figure 12a. Moreover, in a preliminary analysis of the finite element model, the authors attempted to assume perfect bond condition and there was no pinching behavior and strength degradation observed in the analysis results. Hence, a bond-slip model [15] was introduced to the finite element model and the analysis results show that it could predict well the hysteretic behavior of the specimen as presented in Figure 15.

ACI 318-19 [4] code chapter 18.8.2.3 requires joint depth to be greater than twenty times of beam's longitudinal bar diameter (20 d_b) for grade 420 bar and normal weight concrete. This requirement is intended to reduce bond-slip during the formation of plastic hinge in adjacent beams. In this study, the specimen has a joint depth of 400 mm (about 21 d_b) that is slightly above the minimum requirement in the code. Nevertheless, there was still considerable bond-slip in beam's longitudinal reinforcement, and it caused significant pinching behavior. This is in agreement with studies by Leon [3, 16, 17] that suggested specimen with joint depth of 28 d_b had very little strength degradation due to bond-slip while specimen with joint depth of 24 d_b performed remarkably better than those with joint depth of 16 and 20 d_b.

CONCLUSIONS

A comprehensive experimental study regarding the seismic behavior of RC beam-column joint was conducted in the Structural Engineering Laboratory of Petra Christian University. In addition to the experiment, a finite element analysis using VecTor2 software [8] was also performed and the analysis results were compared with the experimental results. From the results, some conclusions can be drawn as follows:

1. The RC beam-column joint specimen failed in beam flexural failure mechanism. The flexural failure of the beams was indicated by crushing of the beam's compression zones located near the joint at the second cycle of 6.00% drift ratio. The nominal moment strength of columns in this study was designed to be much larger (2.5 times) than that of beams so that the columns were not damaged or yielded during the experiment. This was done purposely to investigate bond-slip in beam's reinforcement without being affected by slip in column's reinforcement.
2. The experimental results show that the specimen meets the criteria of ACI 374.1-05 [7] for RC special moment-resisting frames, except the residual stiffness. The specimen tested in this study has residual stiffness of 4.4% and 4.7% in positive and negative directions, respectively, which are slightly below the acceptance criteria of ACI 374.1-05 [7] (5% of initial stiffness). This is mainly due to considerable bond-slip that occurred in beam's longitudinal reinforcement that caused significant pinching behavior.
3. In order to improve the hysteretic behavior of the RC beam-column joint regarding its pinching behavior, a joint depth much greater than ACI 318-19 [4] code provisions is preferred. In this study, the joint depth (about 21 d_b) was slightly greater than the minimum requirement of the code (20 d_b) and it was not sufficient to substantially reduce the amount of bond-slip occurred. As an alternative when the joint depth could not be increased due to design constraints, engineers can use smaller bars to reduce bond-slip in the joint.
4. The finite element analysis using VecTor2 software [8] can simulate well the hysteretic behavior of the RC beam-column joint, including peak strengths, strength degradation, and pinching behavior. Furthermore, the crack patterns can also be reasonably well predicted. From this study, the importance of introducing a bond-slip model [15] was highlighted as the key point to simulate the pinching behavior and strength degradation of the specimen.

ACKNOWLEDGEMENT

This research is a preliminary study of a joint research project between Petra Christian University and P.T. Delta Utracon Synergy. The authors are grateful for the support and funding provided.

REFERENCES

1. Moehle, J., *Seismic Design of Reinforced Concrete Buildings*, McGraw-Hill Education, New York, 2015, 873 pp.
2. Li, Y. and Sanada, Y., Structural Performance Evaluation and Strengthening of An Earthquake-Damaged Beam-Column Joint in Indonesia, *International Conference on Technology, Innovation, and Society 2016*, Padang, Indonesia, 2016, pp. 357-367.
3. Leon, R.T., Interior Joints with Variable Anchorage Lengths, *Journal of Structural Engineering*, *115*(9), 1989, pp. 2261-2275.

4. ACI Committee 318, *Building Code Requirements for Structural Concrete (ACI 318-19) and Commentary*, American Concrete Institute, 2019, 623 pp.
5. ACI Committee 318, *Building Code Requirements for Reinforced Concrete*, American Concrete Institute, 1983, 111 pp.
6. Zhu, S. and Jirsa, J.O., *A Study of Bond Deterioration in Reinforced Concrete Beam-Column Joints*, University of Texas, Austin, 1983, 69 pp.
7. ACI Committee 374, *Acceptance Criteria for Moment Frames Based on Structural Testing and Commentary*, American Concrete Institute, 2005, 13 pp.
8. Vecchio, F., *VecTor2 Basic*, University of Toronto, Toronto, 2021.
9. Vecchio, F.J. and Collins, M.P., Modified Compression-Field Theory for Reinforced Concrete Elements Subjected to Shear, *Journal of the American Concrete Institute*, *83*(2), 1986, pp. 219-231.
10. Vecchio, F., Disturbed Stress Field Model for Reinforced Concrete: Formulation, *ASCE Journal of Structural Engineering*, *126*(9), 2000, pp. 1070-1077.
11. Wong, P.S., Vecchio, F., and Trommels, H., *VecTor2 and FormWorks User's Manual*, Second edition, University of Toronto, Toronto, 2013, 347 pp.
12. Kent, D.C. and Park, R., Flexural Members with Confined Concrete, *ASCE Journal of the Structural Division*, *97*(ST7), 1971, pp. 1970-1990.
13. Seckin, M., *Hysteretic Behaviour of Cast-in-Place Exterior Beam-Column-Slab Subassemblies*, Department of Civil Engineering, University of Toronto, Toronto, 1981.
14. Gan, Y., *Bond Stress and Slip Modeling in Nonlinear Finite Element Analyses of Reinforced Concrete Structures*, Department of Civil Engineering, University of Toronto, Toronto, 2000.
15. Eligehausen, R., Popov, E.P., and Bertero, V.V., *EERC Report 83-23: Local Bond Stress-Slip Relationship of Deformed Bars under Generalized Excitations*, Earthquake Engineering Research Center, University of California, Berkeley, 1983.
16. Leon, R.T., Shear Strength and Hysteretic Behavior of Interior Beam-Column Joints, *ACI Structural Journal*, *87*(1), 1990, pp. 3-11.
17. Leon, R.T., Towards New Bond and Anchorage Provisions for Interior Joints. *ACI Special Publication*, *123*, 1991, pp. 425-442.